BOLETIN DE LA SOCIEDAD ESPAÑOLA DE
Cerámica y Vidrio
A R T I C U L O

Determination of the ionic transport numbers of lanthanum gallate materials by impedance spectroscopy and modified EMF method

J. PEÑA-MARTÍNEZ, D. MARRERO-LÓPEZ, J.C. RUIZ-MORALES, P. NÚÑEZ

Department of Inorganic Chemistry, University of La Laguna, E-38200, Tenerife, Spain.

A combination of impedance spectroscopy and a modified electromotive force method (emf) were used to evaluate the ionic transport numbers and the overall conductivity of several doped lanthanum gallate materials, i.e. $La_{0.9}Sr_{0.1}Ga_{1-x}Mg_xO_{3-\delta}$ (x=0.05-0.30), $La_{0.9}A_{0.1}Ga_{0.8}Mg_{0.2}O_{3-\delta}$ (A=Sr, Ba and Ca) and $La_{0.9}Sr_{0.1}Ga_{0.8}Mg_{0.2-y}Co_yO_{3-\delta}$ (y=0.015 and 0.045). $La_{0.9}Sr_{0.1}Ga_{0.8}Mg_{0.2}O_{2.85}$ (LSGM) sample showed the maximum ionic transport number in the temperature range 900-1173 K, around 0.99 in both O_2/air and H_2/air gradients.

Palabras clave: Conductividad iónica, EMF, LSGM, Número de transporte, SOFC

Determinación de los números de transporte iónico de materiales basados en el galato de lantano mediante técnicas de espectroscopia de impedancia y FEM.

La conductividad total y los números de transporte iónico de las composiciones, basadas en el galato de lantano, $La_{0,9}Sr_{0,1}Ga_{1-x}Mg_xO_{3-\delta}$ (x=0,05-0,30), $La_{0,9}A_{0,1}Ga_{0,8}Mg_{0,2}O_{3-\delta}$ (A=Sr, Ba, Ca) y $La_{0,9}Sr_{0,1}Ga_{0,8}Mg_{0,2-y}Co_yO_{3-\delta}$ (y=0.015; 0,045) fueron estudiadas mediante una combinación de técnicas de espectroscopia de impedancia compleja y fuerza electromotriz (fem). La composición $La_{0,9}Sr_{0,1}Ga_{0,8}Mg_{0,2}O_{2,85}$ (LSGM) presenta el mayor número de transporte iónico, concretamente 0,99 en el rango de temperaturas 900-1173 K, tanto en gradiente de O_2/aire como de H_2/aire.

Keywords: EMF, LSGM, Ionic conductivity, SOFC, Transport number

1. INTRODUCTION

Perovskite-type structure materials, ABO_3, based on lanthanum gallate, $LaGaO_3$, are promising materials for intermediate temperature (873-1073 K) solid oxide fuel cells (SOFCs) (1). Although, some drawbacks related to the formation of secondary phases e.g. $LaSrGaO_4$ and $LaSrGa_3O_7$ in the course of processing of $LaGaO_3$-based materials (2), and the chemical and mechanical compatibility with electrode materials should be overcome (3).

These materials exhibit high oxygen ionic conductivity by substituting lanthanum with alkaline-earth elements (Sr, Ca, Ba) and/or incorporating bivalent metal cations (Mg, Ni) into the gallium sublattice due to an increase of the oxygen vacancy concentration. Furthermore, several computational studies of cation defects in lanthanum gallate based materials reported how divalent and trivalent cations with ionic radii ≤0.8 Å (e.g. Fe, Mn, Sc, etc.) are predicted to substitute preferentially for Ga^{3+} position (4), hence the influence of different B-site substitutions on the transport and physicochemical properties of lanthanum gallate has been studied in order to develop novel materials for electrochemical applications (5,6). However, a negligible electronic conductivity is required for many applications, e.g. dense electrolyte in SOFC technology. For example, Kharton et al. (6) have found that gallium substitution with niobium is not a suitable strategy for obtaining improved oxygen ion-conducting solid electrolytes due to an increase of p-type electronic contribution.

One of the most promising compositions is $La_{0.9}Sr_{0.1}Ga_{0.8}Mg_{0.2}O_{2.85}$ (LSGM) material, which has been investigated as solid electrolyte for intermediate temperature solid oxide fuel cell (IT-SOFC) applications (7,8). LSGM exhibits higher ionic conductivity than the-state-of-the-art yttria stabilised zirconia, with a typical value of 0.1 Scm^{-1} at 1073 K and ionic transport numbers greater than 0.99. (9,10).

On the other hand, Ishihara et al. (5) reported that the introduction of small amounts of cobalt into the gallium sites may result in an increase of the ionic conductivity in LSGM material. Nevertheless, it was also found that the electronic conductivity increased and consequently, the ionic transport number decreased with the increasing of cobalt content. The optimal composition for the cobalt doping was estimated between 5 to 8.5 mol%. The partial electronic and hole conductivity in Co doped $LaGaO_3$ based perovskite oxides were investigated with an ion-blocking method (11) and the transport numbers were estimated by the emf of an H_2-O_2 gas concentration cell (5,11). In the present work, it has been investigated the influence of the Co and Mg substitution for Ga-site on the transport properties of several $LaGaO_3$-based materials using a combination of impedance spectroscopy measurements and a modified emf method (12). Additionally, the incorporation of alkaline-earth cations into the La^{3+} site has been also investigated, i.e. $La_{0.9}A_{0.1}Ga_{0.8}Mg_{0.2}O_{3-\delta}$ (A= Ba, Ca and Sr) compositions. The overall conductivity of the

usual impurities found during the synthesis process of LSGM, i.e. $LaSrGaO_4$, $LaSrGa_3O_7$ was also studied by impedance spectroscopy.

2. EXPERIMENTAL

2.1. Sample preparation

$LaGaO_3$, $LaSrGaO_4$, $LaSrGa_3O_7$, $La_{0.9}Sr_{0.1}Ga_{1-x}Mg_xO_{3-(0.1+x)/2}$ (x=0.05, 0.10, 0.15, 0.20, 0.25 and 0.30), $La_{0.9}A_{0.1}Ga_{0.8}Mg_{0.2}O_{2.85}$ (A= Ba, Ca and Sr) and $La_{0.9}Sr_{0.1}Ga_{0.8}Mg_{0.2-y}Co_yO_{3-\delta}$ (y=0.015 and 0.045) phases have been synthesised by solid-state reaction from stoichiometric amounts of high purity oxides and carbonates. La_2O_3 and MgO were fired at 1273 K for 5 hours in air, before weighing, to remove absorbed water and organic species. The corresponding oxide and carbonate mixture was ground using a ball milling system with acetone and fired at 1173 K for 10 hours in air. Afterwards, the oxide mixture was ball milled again and pressed into pellets at 125 MPa (Ø = 10 mm). Finally, these pellets were sintered at 1623 - 1723 K for 6 hours in air.

2.2. Material characterisation by XRD

X-ray powder diffraction (XRD) patterns were recorded with a Philips X´Pert Pro diffractometer equipped with a primary monochromator, $CuK\alpha_1$ radiation, and a X´Celerator detector. The XRD patterns were collected with a step of 0.016º in the 2θ angular range 5-120º and acquisition time of 3h. Profile matching of the XRD patterns was performed using FullProff and WinPlotr programs (13). The usual parameters were refined: scale factors, background coefficients, zero-points, half-width, pseudo-Voigt and asymmetry parameters for the peak-shape. Atomic parameters were not refined.

2.3. Electrical characterisation by impedance spectroscopy

Impedance spectra measurements were carried out on a 2-electrode arrangement using ~7.5 mm diameter and ~1.5 mm thick dense pellets of the corresponding specimen. The density of these pellets was higher than 95% of the theoretical density estimated from the crystallographic data. Porous platinum electrodes were formed by coating platinum paste on both sides of the pellets and then fired at 1173 K for 1 hour in air. The impedance spectra were measured under air using a frequency response analyser (Solartron 1260) in the frequency range from 0.1 Hz to 1 MHz and with an excitation voltage of 100 mV. Impedance spectra data were fitted with equivalent circuits.

2.4. Determination of the ion transport numbers by a modified emf method

The emf technique is based on the measurement of the open-circuit voltage of a cell placed under a chemical potential gradient (14). For an oxygen concentration cell with negligible electrode polarisation resistance, the oxygen ion transference number can be obtained from the ratio of the measured emf (E_{exp}) and theoretical Nernst voltage (E_{th}):

$$t_o = \frac{E_{exp}}{E_{th}} \qquad [1]$$

where

$$E_{th} = \frac{RT}{4F}\ln\left(\frac{p_2}{p_1}\right) \qquad [2]$$

p_1 and p_2 are the values of the oxygen partial pressure at the electrodes, and E_{th} was determined using a YSZ oxygen sensor, see Fig. 1. The electrode polarisation affects the measured emf of electrochemical cells with mixed ionic-electronic conductors, leading to underestimation of ion transference numbers (15). Some authors (12,16) have proposed modified methods taking into account this effect. These methods are based on a modification of the equivalent circuit proposed by Patterson (17). In this work, the modification suggested by Gorelov (12) has been used. The equivalent circuit for such a cell is illustrated in Fig. 1. The electrical current (I) flowing through this cell may be expressed as:

$$I = \frac{E_{th} - \eta}{R_o + R_e} = \frac{E_{exp}}{R_e} \qquad [3]$$

where η is the sum of the electrode overpotentials, and R_o and R_e are ionic and electronic resistances of the mixed conductor, respectively. At low overpotentials, one can assume a linear dependence of overpotential on the current (I), and express the effects of electrode overpotentials in terms of a polarisation resistance (R_η) as:

$$\eta = IR_\eta \qquad [4]$$

The oxygen-ion transference number may be expressed using the quantities R_o and R_e:

$$t_o = \frac{\sigma_o}{\sigma_o + \sigma_e} = \frac{R_e}{R_o + R_e} \qquad [5]$$

where σ_o and σ_e are the ionic and electronic conductivities, respectively. Substituting Eqs. [4] and [5] into Eq. [3], one obtains:

$$E_{exp} = t_o E_{th}\left(1 + \frac{R_\eta}{R_o + R_e}\right)^{-1} \qquad [6]$$

Gorelov proposed studying the emf as a function of an external variable resistance (R_M) closing the circuit (16), see Fig. 1. In this case:

$$\frac{E_{th}}{E_{exp}} - 1 = (R_o + R_\eta)\left(\frac{1}{R_e} + \frac{1}{R_M}\right) \qquad [7]$$

Thus, values of R_e could be calculated from a linear dependence fit:

$$\frac{E_{th}}{E_{exp}} - 1 = A\left(\frac{1}{R_M}\right) + B \qquad [8]$$

where $A=(R_o+R_\eta)$ and $B=(R_o+R_\eta)/R_e$ are regression parameters. One should notice that

$$R_e = \frac{A}{B} \qquad [9]$$

therefore, the oxygen ion transference numbers were calculated as:

$$t_o = 1 - t_e = 1 - \frac{R_{total}}{R_e} \qquad [10]$$

where t_e is the electron transference number, and R_{total} is the overall resistance of the sample, measured independently by impedance spectroscopy. Fig. 2 gives an example of the

representation obtained from Eq. [7] for a LSGM sample under O_2/air gradient.

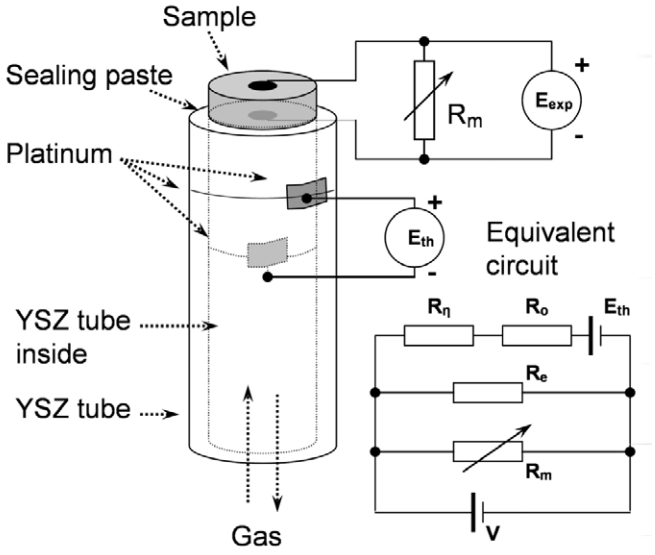

Fig. 1- Scheme of the emf cell and its equivalent circuit, where R_m is the external variable resistance, R_η is the polarisation resistance, R_o and R_e are the ionic and electronic resistances of the mixed conductor, and E_{exp} and E_{th} are the experimental and the theoretical emf values respectively.

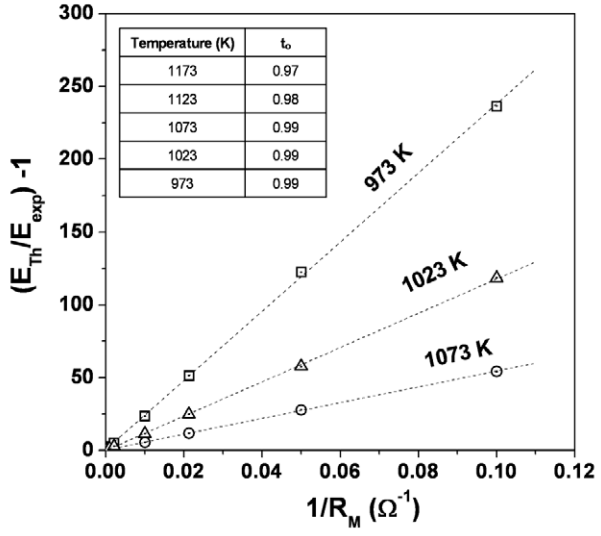

Fig. 2- Experimental data from the modified emf method under O_2/air gradient for a $La_{0.9}Sr_{0.1}Ga_{0.8}Mg_{0.2}O_{2.85}$ sample. Dash line corresponds to the linear fitting to Eq. 7. Table in the inset shows the ionic transport numbers calculated from the different temperatures.

3. RESULTS AND DISCUSSIONS

3.1. Material characterisation by XRD

XRD patterns for $LaGaO_3$, $La_{0.9}Sr_{0.1}Ga_{1-x}Mg_xO_{3-\delta}$ (x=0.05-0.3), and $La_{0.9}Sr_{0.1}Ga_{0.8}Mg_{0.2-y}Co_yO_{3-\delta}$ (y=0, 0.015 and 0.045) are shown in Fig. 3 and 4. The cell parameters and space groups of these compositions are summarised in Table I, and they are in accord with the literature (18). It should be noted that an increase of Mg in the Ga site for $La_{0.9}Sr_{0.1}Ga_{1-x}Mg_xO_{3-\delta}$ compositions produces an increase of the cell parameters, whereas an increase of Co for $La_{0.9}Sr_{0.1}Ga_{0.8}Mg_{0.2-y}Co_yO_{3-\delta}$ compositions is related with a volume cell shrinkage. Another issue to be considered is the presence of impurities as $LaSrGa_3O_7$ and $LaSrGaO_4$ in the Sr-Mg-doped $LaGaO_3$ samples and they are more important in the compositions with Mg content higher than 20 mol% as one can see in Fig. 3. More details about the solubility of Sr and Mg and the phase compositions in the doped $LaGaO_3$ systems can be found elsewhere (19).

TABLE I. LATTICE PARAMETERS OF $LAGAO_3$-BASED MATERIALS.

Composition*	Space group	Lattice parameters (Å)			
		a	b	c	V/Z
$LaGaO_3$	Pnma	5.4917(2)	7.7735(3)	5.5234(2)	58.941(1)
$LSGM_{0.05}$	Imma	5.4992(1)	7.7936(2)	5.5307(1)	59.258(4)
$LSGM_{0.10}$	Imma	5.5048(1)	7.8050(2)	5.5337(1)	59.439(3)
$LSGM_{0.15}$	Imma	5.5103(1)	7.8099(1)	5.5374(1)	59.575(2)
$LSGM_{0.20}$	Imma	5.5218(1)	7.8221(1)	5.5405(1)	59.826(1)
$LSGM_{0.25}$	Imma	5.5211(1)	7.8284(1)	5.5445(1)	59.914(2)
$LSGM_{0.30}$	Imma	5.5267(1)	7.8326(2)	5.5456(1)	60.015(2)
$LSGMC_{0.015}$	Imma	5.5146(1)	7.8146(1)	5.5379(1)	59.664(1)
$LSGMC_{0.045}$	Imma	5.5078(8)	7.8067(8)	5.5369(7)	59.520(1)
LBGM	Pm-3m	3.9217(3)	--	--	60.317(2)
LCGM	Imma	5.5049(1)	7.8033(2)	5.5320(1)	59.410(2)

* $La_{0.9}Sr_{0.1}Ga_{1-x}Mg_xO_{3-\delta}$: $LSGM_x$ (x=0.05-0.30)
$La_{0.9}Sr_{0.1}Ga_{0.8}Mg_{0.2-y}Co_yO_{3-\delta}$: $LSGMC_y$ (y=0.015, 0.045)
$La_{0.9}A_{0.1}Ga_{0.8}Mg_{0.2}O_{2.85}$ (A= Ba,Ca): LBGM, LCGM

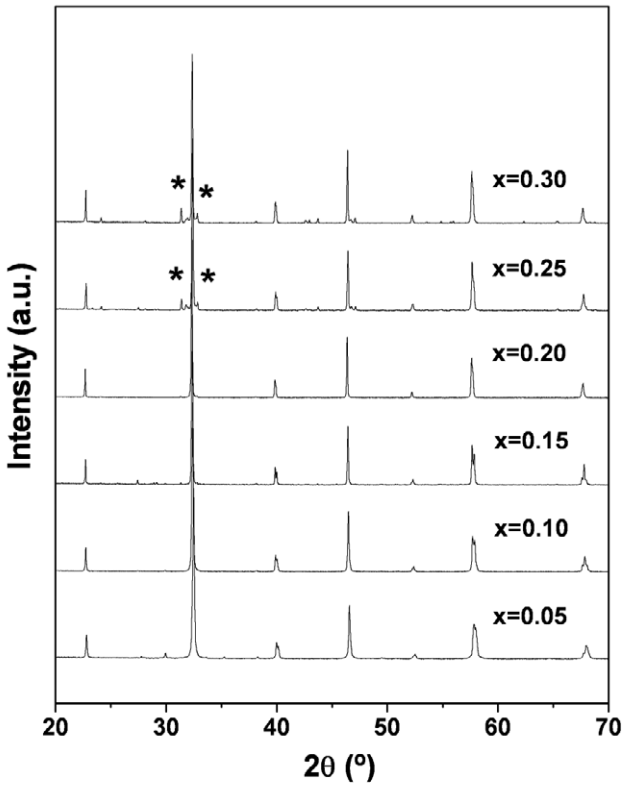

Fig. 3- XRD patterns of $La_{0.9}Sr_{0.1}Ga_{1-x}Mg_xO_{3-(0.1+x)/2}$ samples. $LaSrGa_3O_7$ and $LaSrGaO_4$ impurities are denoted with *.

3.2. Electrical conductivity

The Arrhenius plots for the overall conductivity of $La_{0.9}A_{0.1}Ga_{0.8}Mg_{0.2}O_{2.85}$ (A= Sr, Ba, Ca), $LaSrGaO_4$, $LaSrGa_3O_7$, $La_{0.9}Sr_{0.1}Ga_{1-x}Mg_xO_{3-(0.1+x)/2}$ (x=0.05-0.30) and $La_{0.9}Sr_{0.1}Ga_{0.8}Mg_{0.2-y}Co_yO_{3-\delta}$ (y=0, 0.015-0.045) samples are represented in Fig. 5. $La_{0.9}Sr_{0.1}Ga_{0.8}Mg_{0.2}O_3$ (LSGM) was the composition with higher conductivity in the range 923-1073 K, i.e. 0.1 Scm^{-1} at 1073 K, and $La_{0.9}Sr_{0.1}Ga_{0.8}Mg_{0.155}Co_{0.045}O_{3-\delta}$ the higher one below 923 K, Fig. 5b and c. One should notice the much lower conductivity values of $LaSrGaO_4$ and $LaSrGa_3O_7$ samples compared to LSGM, around six and nine orders less than LSGM, see Fig. 5a. In fact, pure $LaSrGa_3O_7$ is an insulator, however, the oxide-ionic conductivity in $LaSrGa_3O_7$ material has been explained due to an interstitial mechanism considering a different regions with different La/Sr ratios (19), whereas in LSGM material the oxide-ion conductivity has been described by a vacancy mechanism (20). In any case, it is highly recommendable to minimise the formation of $LaSrGaO_4$ and $LaSrGa_3O_7$ impurities during the synthesis of the LSGM material which may seriously affect the performance of LSGM as SOFC electrolyte.

Regarding the overall conductivity of $La_{0.9}A_{0.1}Ga_{0.8}Mg_{0.2}O_{2.85}$ (A=Sr, Ba and Ca) compositions, it can be observed that the conductivity of Sr-substituted composition (LSGM) is comparable to Ba-substituted (LBGM) one, although in the case of LSGM, the conductivity is slightly higher above 770 K. Whereas, the conductivity of Ca-substituted composition (LCGM) is lower than those of Sr and Ba compositions in the whole temperature range studied, possibly due to a decrease of the unit cell parameter after calcium substitution as reported in the literature (10). Therefore, the electrical conductivity of $La_{0.9}A_{0.1}Ga_{0.8}Mg_{0.2}O_{2.85}$ depends on the alkaline earth cations added for the La site and it increases in the order Sr>Ba>Ca. This trend is explained by the lower level of lattice strain upon Sr^{2+} substitution, and it is in a good agreement with the previous work of Ishihara and co-workers (10).

3.3. Ionic transport numbers

The temperature dependence of the ionic transport numbers, estimated by the Gorelov´s method (16), under O_2/air gradient of $La_{0.9}Sr_{0.1}Ga_{1-x}Mg_xO_{3-(0.1+x)/2}$ (x=0.05-0.30), $La_{0.9}A_{0.1}Ga_{0.8}Mg_{0.2}O_{2.85}$ (A= Sr, Ba and Ca) and

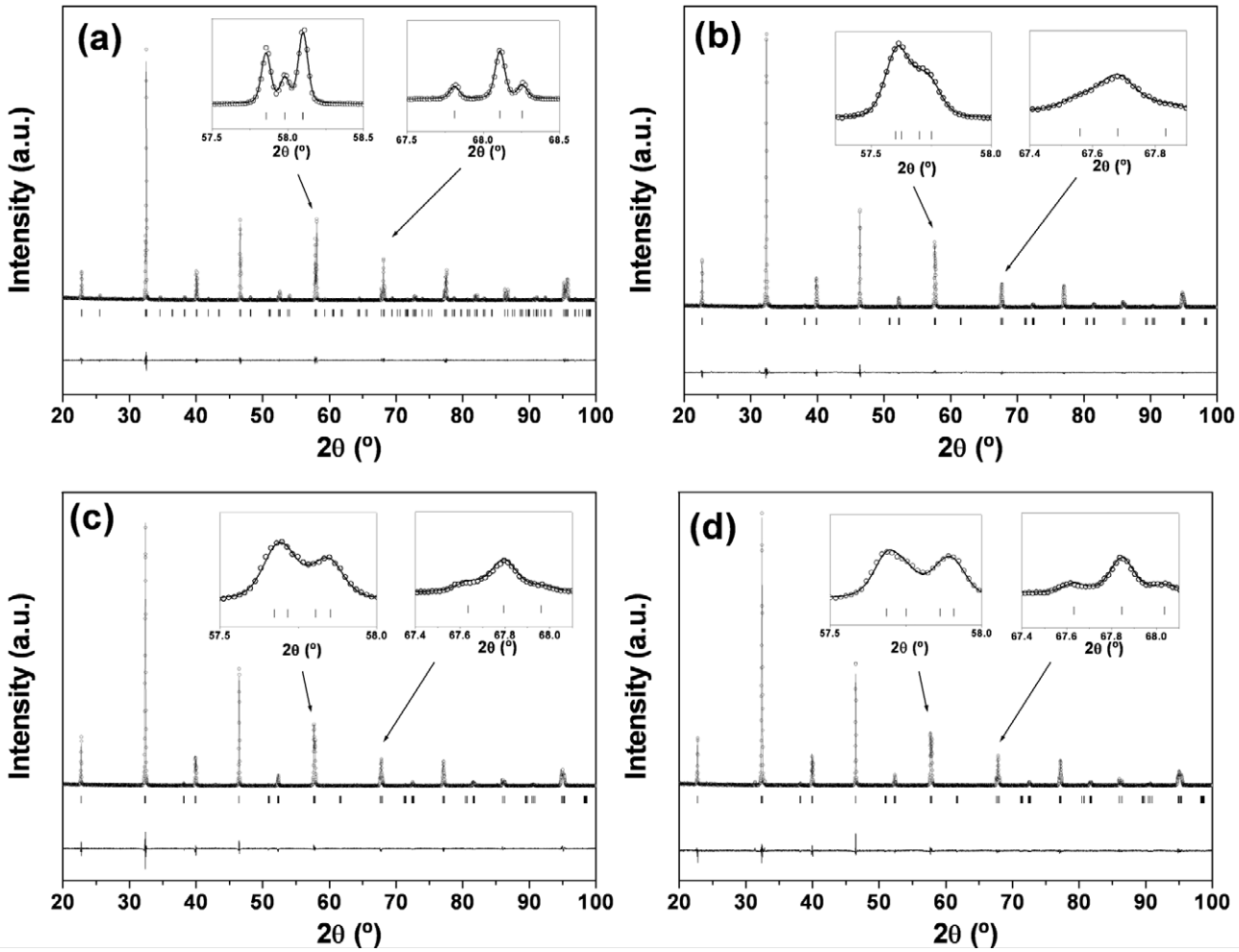

Fig. 4- XRD patterns refined by the Rietveld method at room temperature for (a) $LaGaO_3$, (b) $La_{0.9}Sr_{0.1}Ga_{0.8}Mg_{0.2}O_{2.85}$, (c) $La_{0.9}Sr_{0.1}Ga_{0.8}Mg_{0.185}Co_{0.015}O_{3-\delta}$ and (d) $La_{0.9}Sr_{0.1}Ga_{0.8}Mg_{0.155}Co_{0.045}O_{3-\delta}$.

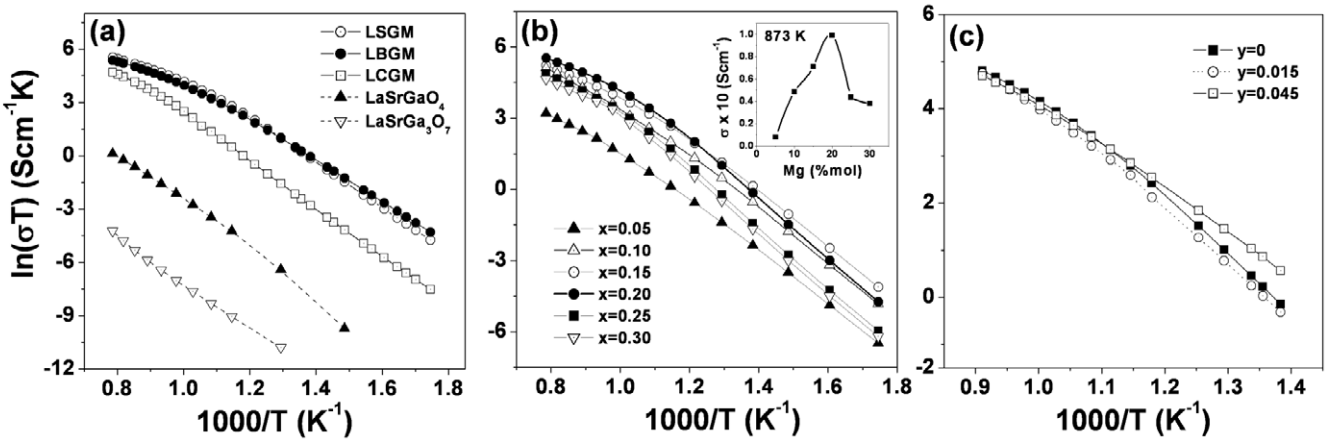

Fig. 5- Arrhenius plot of the overall conductivity, in air, of (a) $La_{0.9}A_{0.1}Ga_{0.8}Mg_{0.2}O_{2.85}$ (A= Sr, Ba and Ca), $LaSrGaO_4$ and $LaSrGa_3O_7$; (b) $La_{0.9}Sr_{0.1}Ga_{1-x}Mg_xO_{3-(0.1+x)/2}$ (x=0.05-0.30); and (c) $La_{0.9}Sr_{0.1}Ga_{0.8}Mg_{0.2-y}Co_yO_{3-\delta}$ (y=0, 0.015 and 0.045). The Inset (b) illustrates the variation of the conductivity as a function of the Mg content at 1073 K.

$La_{0.9}Sr_{0.1}Ga_{0.8}Mg_{0.2-y}Co_yO_{3-\delta}$ (y=0.015-0.045) are shown in Fig. 6. Attending to the substitution of La^{3+} by Sr^{2+}, Ca^{2+} or Ba^{2+}, Sr-based composition showed the highest ionic transport numbers, Fig. 6b. Focus in the Sr-substituted compounds, the maximum ionic transport numbers correspond to the $La_{0.9}Sr_{0.1}Ga_{1-x}Mg_xO_{3-(0.1+x)/2}$ composition with 15 and 20 mol% of Mg. Specifically, the ionic transport numbers under both O_2/air and H_2/air gradient for $La_{0.9}Sr_{0.1}Ga_{0.8}Mg_{0.2}O_3$ (LSGM) composition in the temperature range of 973-1173 K, were around 0.99, as summarised in the inset of Fig. 2. It has to be noticed that all the cobalt-free compositions have an ionic transport number higher than 0.95 under O_2/air gradient. Fig. 6b. Ishihara and co-workers (5) have reported that adding cobalt in Ga site the oxide-ion conductivity can be increased. They studied Sr-Mg doped $LaGaO_3$ compositions with 20 mol% of Sr. In this work, it has been used only 10 mol% of Sr, and as the Sr content increases, the number of the oxygen vacancies is also increased and this possibly affects the electronic contribution of Co-substituted samples. This could explain the different behaviour in the electronic contribution of samples with 10 and 20% Sr. On the other hand, further investigations are needed to clarify how the Sr-content could affect the oxide-ion conductivity of Co-substituted $LaGaO_3$ materials.

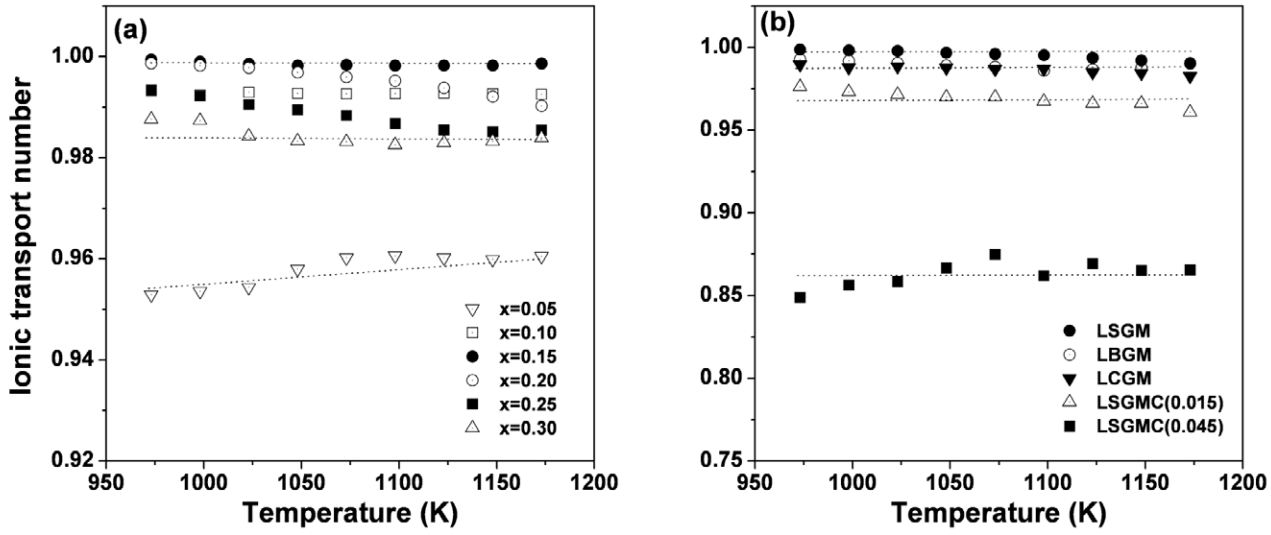

Fig. 6- Ionic transport numbers for (a) $La_{0.9}Sr_{0.1}Ga_{1-x}Mg_xO_{3-(0.1+x)/2}$ (x=0.05-0.30), (b) $La_{0.9}A_{0.1}Ga_{0.8}Mg_{0.2}O_{2.85}$ (A= Sr, Ba and Ca) and $La_{0.9}Sr_{0.1}Ga_{0.8}Mg_{0.2-y}Co_yO_{3-\delta}$ (y=0, 0.015 and 0.045) under O_2/air gradient.

Thus, the substitution of La^{3+} and Ga^{3+} for Sr^{2+} and Mg^{2+} respectively is an effective method for enhancing the oxide-ion conductivity due to the creation of oxygen vacancies in the oxide crystal lattice as indicated in the literature (4).

Otherwise, the ionic transport numbers for Co-substituted $LaGaO_3$ materials decreased as the cobalt content increased,

4. CONCLUSIONS

The ionic transport numbers and the overall conductivity of $La_{0.9}A_{0.1}Ga_{0.8}Mg_{0.2}O_{2.85}$ (A= Sr, Ba and Ca), $La_{0.9}Sr_{0.1}Ga_{1-x}Mg_xO_{3-(0.1+x)/2}$ (x=0.05, 0.10, 0.15, 0.20, 0.25 and 0.30), and $La_{0.9}Sr_{0.1}Ga_{0.8}Mg_{0.2-y}Co_yO_{3-\delta}$ (y=0.015 and

0.045) were determined by a combination of impedance spectroscopy measurements and a modified emf method. $La_{0.9}Sr_{0.1}Ga_{0.8}Mg_{0.2}O_{2.85}$ (LSGM) sample showed the highest overall conductivity at 1073 K, ~0.1 Scm^{-1}, and an ionic transport number around 0.99, in both O_2/air and H_2/air gradients, in the temperature range 773-1073 K, whereas the Co-substituted $La_{0.9}Sr_{0.1}Ga_{0.8}Mg_{0.155}Co_{0.045}O_{3-\delta}$ sample showed a value around 0.85 in O_2/air gradient.

ACKNOWLEDGEMENTS

The authors acknowledge financial support from Spanish Government (MAT2004-3856 project and "Ramón y Cajal" fellowship for J.C. R-M), and Canary Islands Government ("Programa de Incorporación de doctores y tecnólogos a empresas privadas y otras entidades" for D.M-L). The authors are also grateful to Luis Hernández for his technical assistance.

REFERENCES

1. B.C.H. Steele, A. Heinzel, Materials for fuel-cell technologies, Nature, 414, 345-352 (2001).
2. A. Matraszek, L. Singheiser, D. Kobertz, K. Hilpert, M. Miller, O. Schulz, M. Martin, Phase diagram study in the La_2O_3–Ga_2O_3–MgO–SrO system in air, Solid State Ionics, 166, 343-350 (2004).
3. M. Feng, J.B. Goodenough, K. Huang, C. Milliken, Fuel cells with doped lanthanum gallate electrolyte, J. Power Sources, 63, 47-51 (1996).
4. M.S. Islam, R.A. Davies, Atomistic study of dopant site-selectivity and defect association in the lanthanum gallate perovskite, J. Mater. Chem., 14, 86-93 (2004).
5. T. Ishihara, H. Furutani, M. Honda, T. Yamada, T. Shibayama, T. Akbay, N. Sakai, H. Yokokawa, Y. Takita, Improved Oxide Ion Conductivity in $La_{0.8}Sr_{0.2}Ga_{0.8}Mg_{0.2}O_3$ by Doping Co, Chem. Matter., 11, 2081-2088 (1999).
6. V.V. Kharton, A.P. Viskup, A.A. Yaremchenko, R.T. Baker, B. Gharbage, G.C. Mather, F.M. Figueiredo, E.N. Naumovick, F.M.B. Marques, Ionic conductivity of La(Sr)Ga(Mg,M)$O_{3-\delta}$ (M=Ti, Cr, Fe, Co, Ni): effects of transition metal dopants, Solid State Ionics, 132, 119-130 (2000).
7. J. Peña-Martínez, D. Marrero-López, J.C. Ruiz-Morales, C. Savaniu, P. Núñez, J.T.S. Irvine, Anodic Performance and Intermediate Temperature Fuel Cell Testing of $La_{0.75}Sr_{0.25}Cr_{0.5}Mn_{0.5}O_{3-\delta}$ at Lanthanum Gallate Electrolytes, Chem. Matter., 18, 1001-1006 (2006).
8. J. Peña Martínez, D. Marrero-López, D. Pérez-Coll, J.C. Ruiz-Morales, P. Núñez, Performance of XSCoF (X = Ba, La and Sm) and LSCrX ' (X' = Mn, Fe and Al) perovskite-structure materials on LSGM electrolyte for IT-SOFC, Electrochim. Acta, 52 2950-2958 (2007).
9. M. Feng, J.B. Goodenough, A superior oxide-ion electrolyte, Eur. J. Solid State Inorg. Chem., 31, 663-672 (1994).
10. T. Ishihara, H. Matsuda, Y. Takita, Doped $LaGaO_3$ Perovskite Type Oxide as a New Oxide Ionic Conductor, J. Am. Chem. Soc., 116, 3801-3803 (1994).
11. T. Ishihara, S. Ishikawa, C. Yu, T. Akbay, K. Hosoi, H. Nishiguchi, Y. Takita, Oxide ion and electronic conductivity in Co doped $La_{0.8}Sr_{0.2}Ga_{0.8}Mg_{0.2}O_3$ perovskite oxide, Phys. Chem. Chem. Phys., 5, 2257-2263 (2003).
12. V.P. Gorelov, Determination of the transference numbers in ionic conductors by the electromotive force method with an active load, Elektrokhimiya, 24, 1380-1381 (1998).
13. J. Rodríguez-Carvajal, T. Roisnel, FullProf.98 and WinPLOTR: New Windows 95/NT Applications for Diffraction Commission For Powder Diffraction, International Union for Crystallography, Newletter N°20, 1998.
14. C. Wagner, Beitrag zur Theorie des Anlaufvorgangs, Z. Phys. Chem. B., 21, 25 (1933).
15. J.R. Frade, V.V. Kharton, A.A. Yaremchenko, E.V. Tsipis, Applicability of emf measurements under external load resistance conditions for ion transport number determination, J. Solid. State Electrochem., 10, 96-103 (2006).
16. V.V. Kharton, A.P. Viskup, F.M. Figueiredo, E.N. Naumovich, A.A. Yaremchenko, F.M.B. Marques, Electron–hole conduction in Pr-doped Ce(Gd)$O_{2-\delta}$ by faradaic efficiency and emf measurements, Electrochim. Acta, 46, 2879-2889 (2001).
17. J.W. Patterson, In: Brubaker G. et al. (eds). ACS symposium series, no.89, Corrosion Chemistry, p. 96, American Chemical Society, Washington DC, pp. 96, 1979.
18. T. Shibasaki, T. Furuya, S. Wang, T. Hashimoto, Crystal structure and phase transition behavior of $La_{1-x}Sr_xGa_{1-y}Mg_yO_{3-\delta}$, Solid State Ionics, 174, 193-203 (2004).
19. P. Majewski, M. Rozumek, F. Aldinger, Phase diagram studies in the systems La_2O_3–SrO–MgO–Ga_2O_3 at 1350–1400ºC in air with emphasis on Sr and Mg substituted $LaGaO_3$, J. Alloys Compd., 329, 253-258 (2001).
20. R.A. De Souza, J. Maier, A computational study of cation defects in $LaGaO_3$, Phys.Chem. Chem. Phys., 5, 740-748 (2003).

Recibido: 31.07.07
Aceptado: 20.12.07